Chemistry Research Journal, 2019, 4(3):30-42

Available online www.chemrj.org

Research Article

ISSN: 2455-8990
CODEN(USA): CRJHA5

A DFT analysis of the relationships between electronic structure and affinity for dopamine D_2, D_3 and D_4receptor subtypesin a group of 77-LH-28-1 derivatives

Juan S. Gómez-Jeria*, Nicolás Garrido-Sáez

Department of Chemistry, Faculty of Sciences, University of Chile, Las Palmeras 3425, Santiago 7800003, Chile
*Corresponding Author: facien03@uchile.cl

Abstract We have studied the relationships between electronic structure and affinity for D_2, D_3 and D_4 dopamine receptor subtypesin a group of 1-[3-(4-butylpiperidin-1-yl)propyl]-1,2,3,4-tetrahydroquinolin-2-one (77-LH-28-1) derivatives. The Klopman-Peradejordi-Gómez method was employed. Statistically significant results were obtained for all the cases. The analysis of the resulting equations provided data that can be used to design new derivatives with enhanced affinity through appropriate substitutions at selected atoms.

Keywords KPG method, QSAR, dopamine, receptor affinity, DFT, D_2 receptor, D_3 receptor, D_4 receptor, 77-LH-28-1, electronic structure

Introduction

Dopamine is one of the three main signaling molecules from the catecholamine family. The other two are adrenaline and noradrenaline. It is usually recognized for its role in motivation, reward and pleasure, but also plays a critical role in modulating cognitive flexibility, emotional resilience, focus and motivation. Also, dopamine is one of the chief regulators of coordination and motor control of body movements. Up today there are at least five subtypes of dopamine receptors, D_1, D_2, D_3, D_4 and D_5.D_2, D_3 and D_4 receptors are members of the D_2-like family. The dysfunction of the dopaminergic neurotransmission in the central nervous system has been associated with a variety of neuropsychiatric disorders, including for example attention-deficit hyperactivity disorder, drug and alcohol dependence, social phobia Tourette's syndrome an dParkinson's disease. For these reasons dopamine receptors are common drug targets. Antipsychotic drugs are often dopamine receptor antagonists while psychostimulants are typically indirect agonists of dopamine receptors.

In our Unit we have carried out three studies on some molecules interacting with dopamine receptors [1-3]. Recently we have become interested in a group of molecules presenting affinity for three dopamine receptor subtypes and five muscarinic acetylcholine receptors [4]. This provides the possibility of comparing the electronic determinants of receptor affinity within a family of receptors. Here we present the results of a quantum chemical analysis of the relationships between electronic structure and receptor affinity for the case of the dopamine receptors.

Methods, models and calculations

The molecules and their receptor affinities (measured in human cloned D_2, D_3 and D_4 receptors expressed in HEK293T cells)were selected from a recent publication [4]. They are shown in Fig. 1 and Table 1.

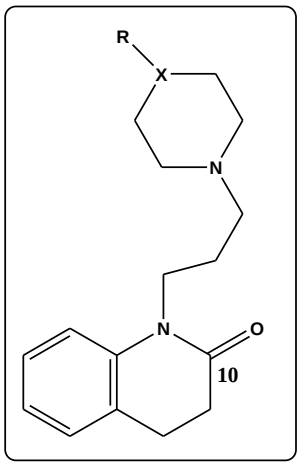

Figure 1: General structure of molecules

Table 1: Dopamine receptor affinities of 77-LH-28-1 derivatives

Mol.	X	R	$pK_i(hD_2R)$	$pK_i(hD_3R)$	$pK_i(hD_4R)$
1	CH	$(CH_2)_3CH_3$	6.17	6.21	9.01
2	CH	CH_3	5.35	5.43	6.59
3	CH	$(CH_2)_2CH_3$	6.04	5.81	8.28
4	CH	$(CH_2)_4CH_3$	6.28	6.55	8.86
5	CH	$(CH_2)_2CH_2OH$	6.18	6.23	7.13
6	CH	$(CH_2)_4CH_2OH$	5.93	6.17	8.36
7	CH	$(CH2)_6CH_2OH$	6.03	6.02	7.00
8	CH	C_6H_5	6.34	6.15	8.71
9	CH	$CH_2C_6H_5$	6.04	5.74	8.90
10	CH	$CH_2CH_2C_6H_5$	6.54	6.39	8.67
11	N	$(CH_2)_3CH_3$	5.29	5.41	6.50
12	N	C_6H_5	5.96	5.88	8.54
13	N	$CH_2C_6H_5$	5.42	5.58	7.70
14	N	$CH_2CH_2C_6H_5$	5.24	5.40	7.54

The wok was carried out employing the Klopman-Peradejordi-Gómez (KPG) method [5]. As the method has been recently reviewed we present here a short summary [6-13]. The drug-receptor affinity constant, K_i, is a linear function of several local atomic reactivity indices (LARIs) and has the following general form:

$$\log K_i = a + bM_{D_i} + c\log\left[\sigma_{D_i}/(ABC)^{1/2}\right] + \sum_j \left[e_j Q_j + f_j S_j^E + s_j S_j^N\right] +$$
$$+ \sum_j \sum_m \left[h_j(m)F_j(m) + x_j(m)S_j^E(m)\right] + + \sum_j \sum_{m'} \left[r_j(m')F_j(m') + t_j(m')S_j^N(m')\right] +$$
$$+ \sum_j \left[g_j\mu_j + k_j\eta_j + o_j\omega_j + z_j\varsigma_j + w_j Q_j^{\max}\right] \quad (1)$$

where M is the drug's mass, σ its symmetry number and ABC the product of the drug's moments of inertia about the three principal axes of rotation. Q_i is the net charge of atom i, S_i^E and S_i^N are, respectively, the total atomic electrophilic and nucleophilic superdelocalizabilities, $F_{i,m}$ ($F_{i,m'}$) is the Fukui index of the occupied (empty) MO m (m') located on atom i. $S_i^E(m)$ is the atomic electrophilic superdelocalizability of MO m on atom i, etc. The total atomic electrophilic superdelocalizability of atom i corresponds to the sum over occupied MOs of the $S_i^E(m)$'s and the total atomic nucleophilic superdelocalizability of atom i is the sum over empty MOs of the $S_i^N(m)$'s. The last bracket in Eq. 1 contains new local atomic reactivity indices obtained directly from Molecular Orbital Theory. μ_j, η_j,

ω_j, ζ_j and Q_j^{max} are, respectively, the local atomic electronic chemical potential, the local atomic hardness, the local atomic electrophilicity, the local atomic softness and the maximal amount of charge atom j can receive. We must note that these new local atomic indices are not the ones developed in conceptual DFT that we consider to be conceptually erroneous.

Since the resolution of the system of linear equations is not possible because we have not enough molecules, we made use of Linear Multiple Regression Analysis (LMRA) techniques to find the best solution. For each case, a matrix containing the dependent variable (the biological activity of each case) and the local atomic reactivity indices of all atoms of the common skeleton as independent variables was built. The Statistica software was used for LMRA [14]. We worked with the *common skeleton hypothesis* stating that there is a definite collection of atoms, common to all molecules analyzed, that accounts for nearly all the biological activity [9]. The action of the substituents consists in modifying the electronic structure of the common skeleton and influencing the right alignment of the drug throughout the orientational parameters [15-17]. It is hypothesized that different parts or this common skeleton accounts for almost all the interactions leading to the expression of a given biological activity. The common skeleton is shown in Fig. 2.

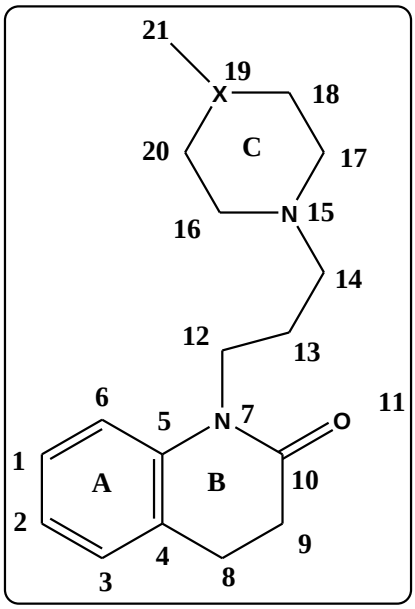

Figure 2: Numbering of the common skeleton

The KPG method has been successful for a large set of different molecules and biological activities [18-22] (and references therein).

The electronic structure of all molecules was calculated with the Density Functional Theory (DFT) at the B3LYP/6-31g(d,p) level after full geometry optimization. The Gaussian suite of programs was used [23]. All the information needed to calculate numerical values for the local atomic reactivity indices was obtained from the Gaussian results with the D-Cent-QSAR software [24]. All the electron populations smaller than or equal to 0.01 e were considered as zero. Negative electron populations coming from Mulliken Population Analysis were corrected as usual [25].

Results

Results for the hD_2R dopamine receptor

The best equation obtained was:

$$pK_i = -60.56 - 4.57S_{12}^{N}(\mathrm{LUMO}+2)^* - 14.24F_{19}(\mathrm{LUMO}+2)^* + \\ +5218.61F_9(\mathrm{LUMO}+1)^* + 0.35S_{21}^{E}(\mathrm{HOMO})^* \quad (2)$$

with n=13, R=0.99, R^2=0.98, adj-R^2=0.98, F(4,8)=124.63 (p<0.000001) and SD=0.06. No outliers were detected and no residuals fall outside the ±2σ limits. Here, S_{12}^{N}(LUMO+2)* is the nucleophilic superdelocalizability of the third lowest empty MO localized on atom 12, F_{19}(LUMO+2)* is the electron population of the third lowest empty MO localized on atom 19, F_9(LUMO+1)* is the electron population of the second lowest MO localized on atom 9 and S_{21}^{E}(HOMO)* is the electrophilic superdelocalizability of the highest occupied MO localized on atom 21. Tables 2 and 3 show the beta coefficients, the results of the t-test for significance of variable and the matrix of squared correlation coefficients for the variables of Eq. 2. There are no significant internal correlations between independent variables (Table 3). Figure 3 displays the plot of observed *vs.* calculated hD_2R affinities.

Table 2: Beta coefficients and t-test for significance of coefficients in Eq. 2

Variable	Beta	t(8)	p-level
S_{12}^{N}(LUMO+2)*	-0.86	-18.002	0.000000
F_{19}(LUMO+2)*	-0.83	-15.83	0.000000
F_9(LUMO+1)*	0.37	7.63	0.00006
S_{21}^{E}(HOMO)*	0.23	4.56	0.0019

Table 3: Matrix of squared correlation coefficients for the variables in Eq. 2

	S_{12}^{N}(LUMO+2)*	F_{19}(LUMO+2)*	F_9(LUMO+1)*
S_{12}^{N}(LUMO+2)*	1.00		
F_{19}(LUMO+2)*	0.01	1.00	
F_9(LUMO+1)*	0.08	0.04	1.00
S_{21}^{E}(HOMO)*	0.00	0.19	0.00

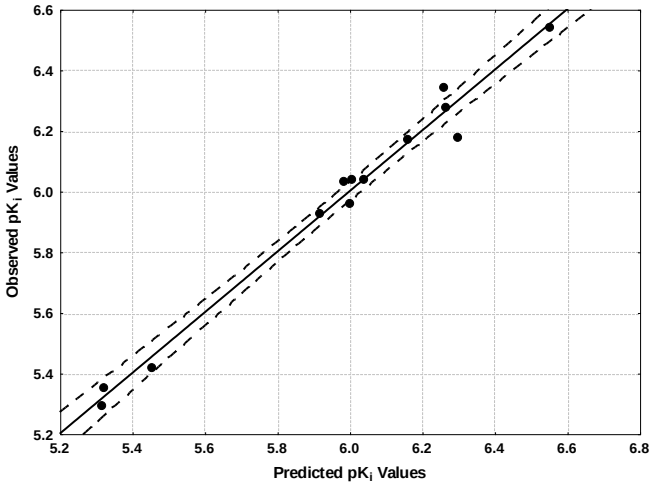

Figure 3: Plot of predicted vs. observed pK_i values (Eq. 2). Dashed lines denote the 95% confidence interval

The associated statistical parameters of Eq. 2 indicate that this equation is statistically significant and that the variation of the numerical values of a group of four local atomic reactivity indices of atoms of the common skeleton explains about 98% of the variation of the pK_i.Figure 3, spanning about 1.3 orders of magnitude, shows that there is a good correlation of observed *versus* calculated values and that almost all points are inside the 95% confidence interval.

Results for the hD_3R dopamine receptor.

The best equation obtained was:

$$pK_i = 235.75 - 1672.91Q_3 - 3859.50F_{10}(HOMO)^* + 9.80S_{13}^{E}(\mathrm{HOMO})^* + \\ + 3028.40F_9(\mathrm{LUMO}+1)^* \quad (3)$$

with n=14, R=0.98, R^2=0.95, adj-R^2=0.93, F(4,9)=45.163 (p<0.00001) and SD=0.10. No outliers were detected and no residuals fall outside the ±2σ limits. Here,Q_3 is the net charge of atom 3, F_{10}(HOMO)* is the Fukui index of the

highest occupied molecular orbital localized on atom 10, S_{13}^{E}(HOMO)* is the electrophilic superdelocalizability of the highest occupied MO localized on atom 13 and F_9(LUMO+1)* is the electron population of the second lowest empty MO localized on atom 9.Tables 4 and 5 show the beta coefficients, the results of the t-test for significance of variable and the matrix of squared correlation coefficients for the variables of Eq. 3. There are no significant internal correlations between independent variables (Table 5). Figure 4 displays the plot of observed *vs.* calculatedhD_3R affinities.

Table 4: Beta coefficients and t-test for significance of coefficients in Eq. 3

Variable	Beta	t(9)	p-level
Q_3	-0.75	-9.65	0.000005
F_{10}(HOMO)*	-0.66	-8.54	0.00001
S_{13}^{E}(HOMO)*	0.35	4.49	0.0015
F_9(LUMO+1)*	0.21	2.86	0.02

Table 5: Matrix of squared correlation coefficients for the variables in Eq. 3

	Q_3	F_{10}(HOMO)*	S_{13}^{E}(HOMO)*	F_9(LUMO+1)*
Q_3	1.00			
F_{10}(HOMO)*	-0.21	1.00		
S_{13}^{E}(HOMO)*	-0.31	0.24	1.00	
F_9(LUMO+1)*	-0.05	0.22	-0.04	1.00

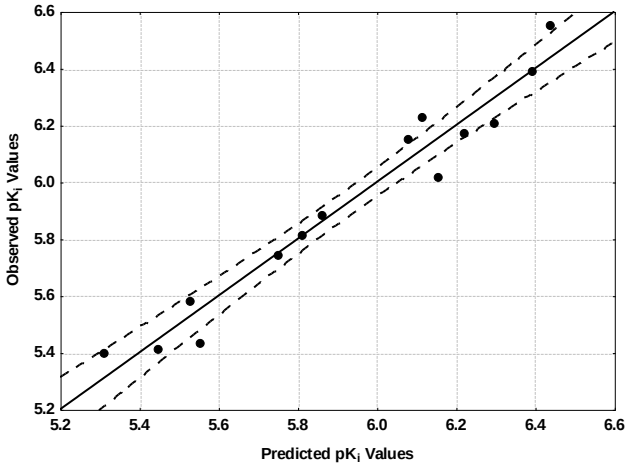

Figure 4: Plot of predicted vs. observed pK_i values (Eq. 3). Dashed lines denote the 95% confidence interval

The associated statistical parameters of Eq. 3 indicate that this equation is statistically significant and that the variation of the numerical values of a group of four local atomic reactivity indices of atoms of the common skeleton explains about 93% of the variation of the pK_i. Figure 4, spanning about 1.1 order of magnitude, shows that there is a good correlation of observed *versus* calculated values and that almost all points are inside the 95% confidence interval or close to it.

Results for the hD_4R dopamine receptor

The best equation obtained was:

$$pK_i = -27.19 + 49.90Q_{17}^{\max} - 13.35S_9^{E}(\mathrm{HOMO}-2)^* + 49.02F_{18}(\mathrm{LUMO})^* + 1.35S_{15}^{N} \quad (4)$$

with n=14, R=0.97, R^2=0.95, adj-R^2=0.92, F(4,9)=40.747 (p<0.00001) and SD=0.24. No outliers were detected and no residuals fall outside the ±2σ limits. Here, $Q_{17}^{\max}$ is the maximal amount of charge atom 17 may receive (Fig. 2), S_9^{E}(HOMO-2)* is the electrophilic superdelocalizability of the third highest occupied local MO of atom 9,

F_{18}(LUMO)* is the electron population of the lowest empty local MO of atom 18 and S_{15}^{N} is the total atomic nucleophilic superdelocalizability of atom 15.Tables 6 and 7 show the beta coefficients, the results of the t-test for significance of variable and the matrix of squared correlation coefficients for the variables of Eq. 4. There are no significant internal correlations between independent variables (Table 7). Figure 5 displays the plot of observed *vs.* calculated hD_4R affinities.

Table 6: eta coefficients and t-test for significance of coefficients in Eq. 4

Variable	Beta	t(9)	p-level
Q_{17}^{max}	1.06	11.55	0.000001
S_9^{E}(HOMO-2)*	-0.54	-5.77	0.0003
F_{18}(LUMO)*	0.38	4.45	0.001
S_{15}^{N}	0.33	3.90	0.004

Table 7: Matrix of squared correlation coefficients for the variables in Eq. 4

	Q_{17}^{max}	S_9^{E}(HOMO-2)*	F_{18}(LUMO)*	S_{15}^{N}
Q_{17}^{max}	1.00			
S_9^{E}(HOMO-2)*	0.53	1.00		
F_{18}(LUMO)*	0.27	0.34	1.00	
S_{15}^{N}	-0.30	-0.34	-0.35	1.00

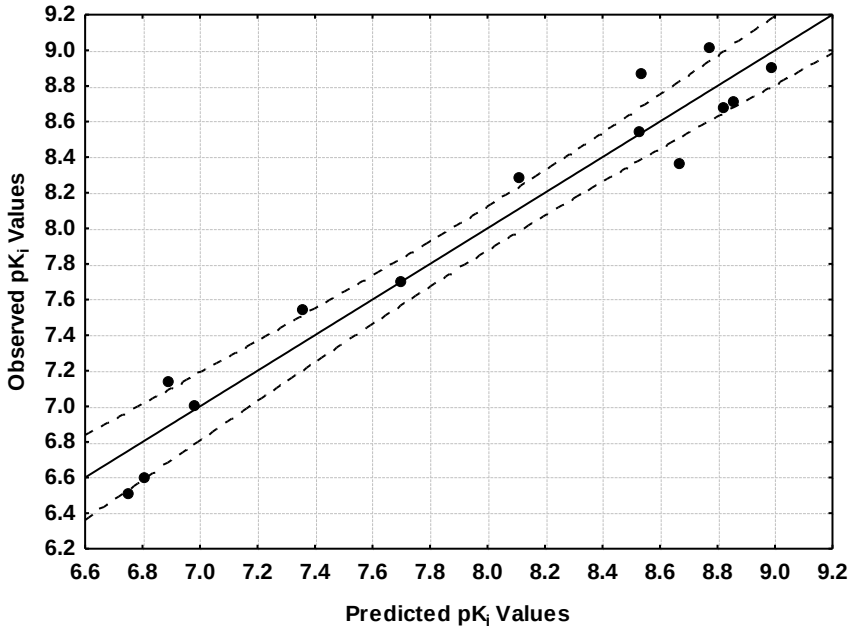

Figure 5: Plot of predicted vs. observed pK_i values (Eq. 4). Dashed lines denote the 95% confidence interval

The associated statistical parameters of Eq. 4 indicate that this equation is statistically significant and that the variation of the numerical values of a group of four local atomic reactivity indices of atoms of the common skeleton explains about 92% of the variation of the pK_i. Figure 5, spanning about 2.5 orders of magnitude, shows that there is a good correlation of observed *versus* calculated values.

Local Molecular Orbitals

The set of *local* molecular orbitals of a given atom is built by considering only those occupied and empty molecule's MOs that are localized on this atom. Therefore, atom x has its own set of local MOs: $(HOMO)_x^*$, $(HOMO-1)_x^*$, $(HOMO-2)_x^*$,…, $(LUMO)_x^*$, $(LUMO+1)_x^*$, $(LUMO+2)_x^*$,...This implies that when a *local* atomic reactivity index of an inner occupied MO (i.e., (HOMO-1)* and/or (HOMO-2)*) or of a higher vacant MO ((LUMO+1)* and/or (LUMO+2)*) appears in any equation, the remaining of the upper occupied MOs (for example, if (HOMO-2)*

appears, upper means (HOMO-1)* and (HOMO)*) or the remaining of the empty MOs (for example, if (LUMO+1)* appears, lower means the (LUMO)*) must contribute to the interaction. Their absence in the equation only means that the variation of their numerical values does not account for the variation of the numerical value of the biological property.Tables 8 and 9 display the local molecular orbital structure of all atoms appearing in Eq. 1-3. Nomenclature of the Tables: Molecule (HOMO number) / (HOMO-2)* (HOMO-1)* (HOMO)* - (LUMO)* (LUMO+1)* (LUMO+2)*.

Table 8: Local molecular orbitals of atoms 4, 9, 10 and 12

Mol.	Atom 4 (C)	Atom 9 (C)	Atom 10 (C)	Atom 12(C)
1 (90)	87π88π89π- 91π92π93π	87σ88σ89σ– 91σ92σ93σ	87σ88σ89π– 91π92π93π	88σ89σ90σ– 93σ96σ97σ
2 (78)	75π76π77π- 79π80π81π	75σ76σ77σ– 79σ80σ 81σ	74π76σ77π– 79π80π 81π	76σ77σ78σ- 81σ84σ85σ
3 (86)	83π84π85π- 87π88π89π	83σ84σ85σ - 87σ88σ89σ	83σ84σ85π- 87π88π89π	84σ85σ86σ - 89σ92σ94σ
4 (94)	91π92π93π- 95π96π97π	91σ92σ93σ- 95σ96σ97σ	91σ92σ93π- 95π96π 97π	92σ93σ94σ- 97σ101σ107σ
5 (90)	87π88π89π- 91π92π93π	87σ88σ89σ- 91σ92σ93σ	87σ88σ89π- 91π92π 93π	88σ89σ90σ- 93σ97σ102σ
6 (98)	95π96π97π- 99π100π101π	95σ96σ97σ- 99σ100σ101σ	95σ96σ97π- 99π100π101π	96σ97σ98σ- 101σ106σ112σ
7(106)	103π104π105π 107π108π109π	103σ104σ105σ- 107σ108σ109σ	103σ104σ105π- 107π108π109π	104σ105σ106σ- 109σ114σ121σ
8 (94)	89π90π93π- 95π96π99π	89σ90σ93σ- 95σ96σ99σ	89σ90σ93π- 95π96π 99π	90σ93σ94σ- 99σ102σ104σ
9 (98)	93π94π97π- 99π100π103π	93σ94σ97σ- 99σ100σ103σ	93σ94σ97π- 99π100π103π	94σ97σ98σ- 103σ107σ112σ
10 (102)	97π98π101π- 103π104π107π	97σ98σ101σ- 103σ104σ107σ	97σ98σ101π- 103π104π107π	98σ101σ102σ- 107σ110σ115σ
11 (90)	86π87π88π- 91π92π93π	86σ87σ88σ- 91σ92σ93σ	86σ87σ88π- 91π92π 93π	87σ88σ89σ- 93σ96σ103σ
12 (94)	89π90π92π- 95π96π99π	84σ89σ90σ- 95σ96σ99σ	89σ90σ92π- 95π96π 99π	90σ92σ93σ- 99σ101σ104σ
13 (98)	92π93π96π- 99π100π103π	88σ92σ93σ- 99100σ103σ	92σ93σ96π- 99π100π103π	93σ96σ98σ- 103σ105σ111σ
14 (102)	96π97π100π103π 104π107π	96σ97σ100σ- 103σ104σ107σ	96σ97σ100π- 103π104π107π	97σ100σ101σ- 107σ110σ117σ

Table 9: Local molecular orbitals of atoms 15, 17, 19 and 21

Mol.	Atom 15 (N)	Atom 17 (C)	Atom 18 (C)	Atom 19 (C or N)	Atom 21
1 (90)	85σ86σ90σ- 98lp99σ100lp	85σ86σ90σ– 96σ97σ99σ	85σ86σ90σ– 98σ100σ101σ	84σ85σ86σ- 103σ105σ106σ	84σ85σ86σ– 96σ97σ105σ
2 (78)	73σ74σ78σ– 86σ88σ91σ	73σ74σ78σ - 85σ86σ89σ	73σ74σ78σ - 86σ90σ92σ	72σ73σ74σ - 86σ92σ94σ	72σ73σ74σ– 85σ90σ91σ
3 (86)	81σ82σ86σ- 94lp95σ98σ	81σ82σ86σ - 94σ95σ97σ	81σ82σ86σ - 94σ98σ99σ	80σ 81σ82σ– 97σ98σ99σ	80σ81σ82σ– 94σ97σ98σ
4 (94)	89σ90σ94σ-	89σ90σ94σ-	89σ90σ94σ-	88σ89σ90σ-	88σ89σ90σ–

	103lp104lp109σ	100σ101σ103σ	102σ103σ105σ	107σ109σ111σ	100σ103σ108σ
5 (90)	84σ85σ90σ- 99lp100σ103σ	84σ85σ90σ- 99σ100σ103σ	84σ85σ90σ- 98σ99σ104σ	83σ84σ85σ- 95σ101σ103σ	83σ84σ85σ– 94σ99σ102σ
6 (98)	92σ93σ98σ- 107lp109lp114σ	92σ93σ98σ- 105σ106σ108σ	92σ93σ98σ- 107σ109σ110σ	91σ92σ93σ- 103σ112σ114σ	91σ92σ93σ– 105σ114σ116σ
7 (106)	100σ101σ106σ- 116lp120σ125σ	100σ101σ106σ- 116σ117σ119σ	100σ101σ106σ- 115σ116σ121σ	99σ100σ101σ- 120σ121σ122σ	99σ100σ101σ- 116σ123σ124σ
8 (94)	88σ92σ94σ- 107σ108σ112π	87σ88σ94σ- 102σ103σ104σ	87σ88σ94σ- 106σ108σ112σ	87σ88σ92σ- 97σ100σ107σ	91π92π94π– 97π98π104π
9 (98)	91σ92σ98σ- 104lp109lp114σ	91σ92σ98σ- 106σ107σ108σ	92σ96σ98σ- 104σ117σ118σ	91σ92σ96σ- 101σ102σ104σ	91σ92σ96σ– 101σ106σ107σ
10 (102)	95σ96σ102σ- 111lp113lp114σ	95σ96σ102σ- 113σ114σ115σ	95σ96σ102σ- 111σ112σ113σ	94σ95σ96σ- 114σ115σ116σ	94σ95σ96σ– 111σ113σ116σ
11 (90)	88lp89σ90σ- 94σ100lp103σ	84σ89σ90σ- 98σ99σ100σ	84σ89σ90σ- 100σ101σ102σ	84σ89σ90σ- 94σ103σ105σ	83σ84σ90σ– 98σ101σ102σ
12 (94)	88lp92lp93σ- 105σ106σ107lp	86σ88σ93σ- 103σ104σ107σ	88σ93σ94σ- 97σ98σ101σ	86σ88σ94σ- 98σ102σ110σ	86π88π94π– 97π98π105π
13 (98)	96lp97σ98σ– 110lp111σ116lp	90σ97σ98σ- 108σ109σ111σ	95σ97σ98σ- 109σ111σ114σ	95σ97σ98σ- 109σ113σ117σ	90σ95σ97σ– 101σ105σ106σ
14 (102)	100lp101σ102σ- 108lp112lp114lp	99σ101σ102σ- 113σ114σ115σ	94σ101σ102σ- 114σ115σ117σ	99σ101σ102σ- 106σ117σ119σ	99σ101σ102σ- 106σ108σ112σ

Discussion

Discussion of the D_2 dopamine receptor results

Table 2 shows that the importance of variables in Eq. 2 is S_{12}^{N}(LUMO+2)* ~ F_{19}(LUMO+2)* >> F_9(LUMO+1)* > S_{21}^{E}(HOMO)*. The analysis of Eq. 2 shows that a high receptor activity is associated with small (positive) values of S_{12}^{N}(LUMO+2)* and F_{19}(LUMO+2)*, large values of F_9(LUMO+1)* and large (negative) numerical values for S_{21}^{E}(HOMO)*.Atom 12 is a saturated carbon in the chain linking rings B and C (Fig. 2). Table 8 shows that all local MOs have a σ nature and also that $(LUMO)_{12}^{*}$ does not coincide with the molecule's LUMO. Small positive values for S_{12}^{N}(LUMO+2)* are obtained by raising the corresponding eigenvalue, making this MO less reactive and suggesting that the empty MOs of this atom are not interacting with an electron-rich center. On the other hand, $(HOMO)_{12}^{*}$ coincides with the molecule's LUMO in almost all cases and in the remaining ones they coincide with the molecular (HOMO-1). This suggests that atom 21 could be interacting with an electron-deficient center of σ nature, without ruling out the possibility of σ-π or σ-cation interactions. Atom 19 can be a saturated C or an N atom inside saturated ring C (Fig. 2). Table 9 shows that only in the case of molecules with X=N (Table 1) the local $HOMO_{19}^{*}$ coincides with the molecular one. In all the other cases neither $HOMO_{19}^{*}$ nor $LUMO_{19}^{*}$ coincide with the molecular frontier MOs and are energetically very 'far' from them. All local MOs have σ nature. Small (positive) values of F_{19}(LUMO+2)* are associated with high affinity. These values can be obtained by diminishing the virtual electron population of $(LUMO+2)_{19}^{*}$, making this MO less reactive. Given the abovementioned energy situation of the frontier local MOs we shall comment on those cases in which the local $HOMO_{19}^{*}$ coincides with the molecular one. In this case it is more probable that these atoms interact with an electron-deficient center. In this case, the receptor affinity can be increased by substitutions that help to localize the molecular HOMO on atom 19. This seems to be the most probable hypothesis. The interaction can be of the σ-σ, σ-π or σ-cation kinds. Atom 9 is a saturated carbon in ring B (Fig. 2). Table 8 shows that all local MOs have σ nature. The local $(LUMO)_9^{*}$ coincides with the molecular LUMO in all cases. In the cases of molecules with X=CH (Table 1) the local $(LUMO)_9^{*}$ coincides with (LUMO-1) and in the cases when X=N the local $(LUMO)_9^{*}$ coincides with inner occupied molecular MOs. Large values of F_9(LUMO+1)* are associated with high affinity. This indicates that atom 9 is prone to interact with electron-rich centers, through at least its two lowest empty MOs. The electron-rich center may contain σ or π

electrons or be an anion.Atom 21 is the first atom of the substituent attached to atom 19 (Fig. 2). In all but two cases this is a saturated carbon atom. In the other two cases we are dealing with an aromatic carbon atom. Table 9 shows that all MOs have σ nature with the exception of molecules 8 and 12. Large (negative) numerical values for S_{21}^{E}(HOMO)* are required for high affinity. These values are obtained by 'moving' the energy of the HOMO towards zero, making this MO more reactive. Therefore we suggest that atom 21 is interacting with an electron-deficient center and that the nature (π or σ) of the MOs seems not to be important, pointing to a σ-cation or π-cation interaction. All the suggestions are displayed in the partial 2D pharmacophore of Fig. 6.

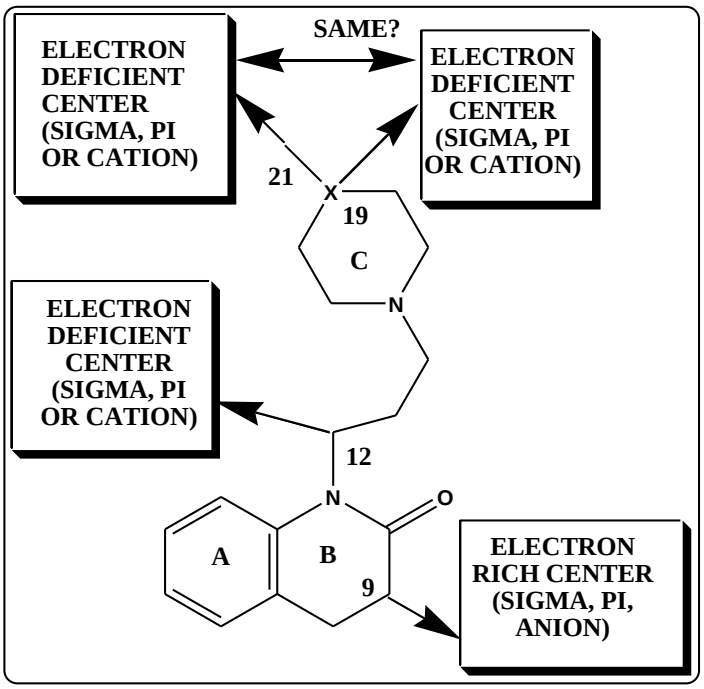

Figure 6: Partial 2D pharmacophore for D_2 dopamine receptor affinity

Discussion of the D_3 dopamine receptor results

Table 4 shows that the importance of variables in Eq. 3 isQ_3>F_{10}(HOMO)*>> S_{13}^{E}(HOMO)* > F_9(LUMO+1)*.A high receptor affinity is associated witha positive net charge on atom 3, a small value of the electron population of $(HOMO)_{10}^{*}$, a small (negative) value for S_{13}^{E}(HOMO)* and a large virtual electron population in $(LUMO+1)_{9}^{*}$.Atom 3 is an aromatic carbon in ring A (Fig. 2).A high receptor affinity is associated with a positive net charge on this atom. This suggests the possible existence of an electrostatic interaction between atom 3 and a positively charged site. Atom 10 is a carbon in ring B (Fig. 2). A high receptor affinity is associated with a small value of the electron population of $(HOMO)_{10}^{*}$. Table 8 shows that $(LUMO)_{10}^{*}$ coincides in all cases with the molecular LUMO and that $(HOMO)_{10}^{*}$ coincides with inner occupied molecular MOs. The ideal situation will be the case when the local $(HOMO)^{*}$ coincides with, for example, (HOMO-4) or with an even more internal molecular MO. This suggests that atom 10 is interacting with an electron-rich center. This interaction can be of π-π, π-σ or π-anion kind. Atom 13 is a saturated carbon in the chain linking rings B and C (Fig. 2).All MOs have a σ nature. Given that a small (negative) value for S_{13}^{E}(HOMO)* is associated with high affinity, we suggest that atom 13 is interacting with an electron-rich center because small (negative) values for this index are obtained by making it less reactive (by changing it by an even more internal molecular MO or by making more negative the MO energy). The interaction can be of σ-σ, σ-π or σ-anion kind. Atom 9 is a saturated carbon in ring B (Fig. 2). Table 8 shows that all local MOs have σ nature. Considering that a large virtual electron population in $(LUMO+1)_{9}^{*}$ is associated with high affinity and that this requirement is the same in Eq. 1, we suggest that atom 9 is susceptible to interact with electron-

rich centers, through at least its two lowest empty MOs. The electron-rich center may contain σ or π electrons or be an anion. All the suggestions are displayed in the partial 2D pharmacophore of Fig. 7.

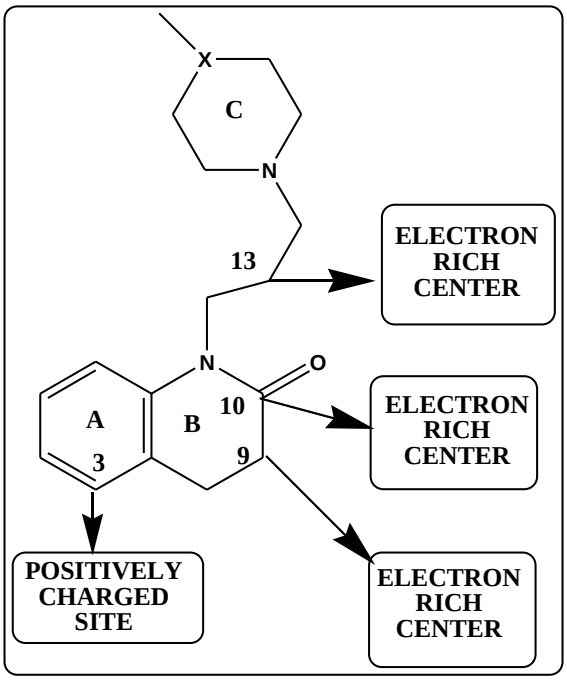

Figure 7: Partial 2D pharmacophore for D_3 dopamine receptor affinity

Discussion of the D_4 dopamine receptor results

Table 6 shows that the importance of variables in Eq. 4 is Q_{17}^{max}>>S_9^E(HOMO-2)*> F_{18}(LUMO)*~ S_{15}^N.A high receptor affinity is associated with a high value for Q_{17}^{max}, a high (negative) value of S_9^E(HOMO-2)*, a high electron population at $(LUMO)_{18}^*$ and a high value for S_{15}^N.

Atom 17 is a saturated carbon in ring C (Fig. 2). Table 9 shows that all MOs are of σ nature, that in all but one case the local $(HOMO)_{17}$* coincides with the molecular HOMO and that all local $(LUMO)_{17}^*$ coincide with higher empty molecular MOs. A high receptor affinity is associated with a high value for Q_{17}^{max}. This suggests that atom 17 should be prone to receive charge or at least to interact with an electron-rich center. Therefore, an ideal situation will be when $(HOMO)_{17}$* coincides with inner occupied molecular MOs and when $(LUMO)_{17}^*$ coincide with the molecular LUMO. The interaction can be of σ-σ, σ-π or σ-anion kind.

Atom 9 is a saturated carbon in ring B (Fig. 2). All MOs have aσ nature (Table 8). A high (negative) value of S_9^E(HOMO-2)* is associated with high receptor affinity. Remembering that $S_9^E(\text{HOMO-2})^* = F_9(\text{HOMO-2})^*/E_{(\text{HOMO-2})_9^*}$, where $E_{(\text{HOMO-2})_9^*}$ is the energy of $(HOMO-2)_9$*, we can obtain large values for this index by shifting the MO energy upwards, i.e., toward zero. This will produce a $(HOMO-2)_9$* more reactive and also a more reactive $(HOMO-1)_9$* and $(HOMO)_9$*. Therefore, it is suggested that atom 9 is interacting with an electron-deficient center.The interaction can be of σ-σ, σ-π or σ-cation kind.

Atom 18 is a saturated carbon in ring C (Fig. 2). Table 9 shows that all local MOs have aσ nature and that all local (HOMO)* coincide with the molecular HOMO. Local (LUMO)* coincide with inner empty molecular MOs. A high receptor affinity is associated with a high electron population at $(LUMO)_{18}^*$. This indicates that this atom could be interacting with an electron-rich center. The interaction can be of σ-σ, σ-π or σ-anion kind.

Atom 15 is a nitrogen in ring C (Fig. 2). Table 9 shows that all local MOs have aσ or lone pair (lp) nature. A high receptor affinity is associated with a high value for S_{15}^N.Knowingthat $S_{15}^N = \sum_{MO=LUMO}^{N} (F_{15}(MO)/E_{MO})$,we can see that the contributions of the lowest empty MOs are numerically more important (this because the MO energy

value). To obtain larger values for this index, we must shift downwards the MO energy (i.e., toward zero) making empty MOs more reactive. On the other hand and considering the fact that $(LUMO)_{15}^{*}$ coincides with higher empty molecular MO in all the molecules, a faster way to obtain larger values for this index consists in making $(LUMO)_{15}^{*}$ coincide with the molecular LUMO. Therefore, we suggest that atom 15 is interacting with an electron-rich center. The interaction can be of σ-σ, σ-π or σ-anion kind. All the suggestions are displayed in the partial 2D pharmacophore of Fig. 8.

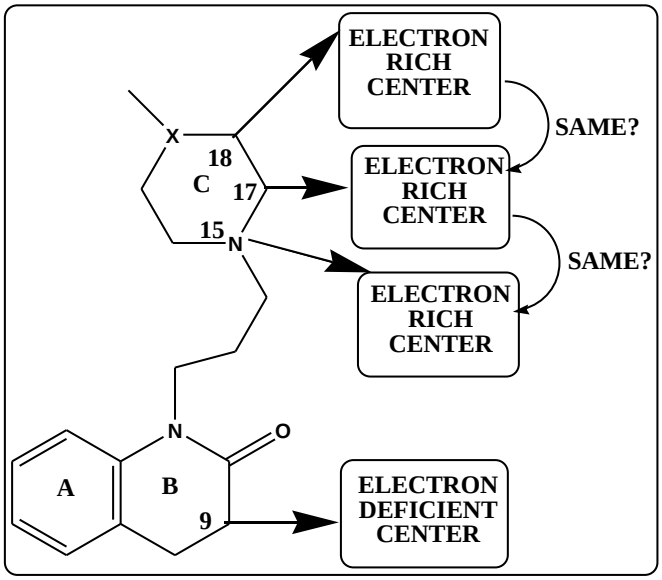

Figure 8: Partial 2D pharmacophore D_4 dopamine receptor affinity

. A very interesting fact is that the results show that sigma electrons play a role in the drug-receptor interaction. This phenomenon appeared in previous studies on other molecules and receptors. Now that we have docking tools it is easy to see how the sigma electrons of the drugs interact with their sites but, as far as we know, the KPG method is the only one producing results containing these interactions.

In summary, we have obtained statistically significant equations relating electronic structure with receptor affinity for D_2, D_3 and D_4 subtypes of dopamine receptors. They should allow medicinal chemists to select target atoms and appropriate substituent's to obtain molecules with enhanced receptor affinity.

References

[1]. Gómez-Jeria, J. S.; Valdebenito-Gamboa, J. A Density Functional Study of the Relationships between Electronic Structure and Dopamine D_2 receptor binding affinity of a series of [4-(4-Carboxamidobutyl)]-1-arylpiperazines. *Research Journal of Pharmaceutical, Biological and Chemical Sciences* 2015, 6, 203-218.

[2]. Gómez-Jeria, J. S.; Valdebenito-Gamboa, J. Electronic structure and docking studies of the Dopamine D_3 receptor binding affinity of a series of [4-(4-Carboxamidobutyl)]-1-arylpiperazines. *Der Pharma Chemica* 2015, 7, 323-347.

[3]. Gómez-Jeria, J. S.; Ojeda-Vergara, M. Electrostatic medium effects and formal quantum structure-activity relationships in apomorphines interacting with D_1 and D_2 dopamine receptors. *International Journal of Quantum Chemistry* 1997, 61, 997-1002.

[4]. Del Bello, F.; Bonifazi, A.; Giorgioni, G.; Cifani, C.; Micioni Di Bonaventura, M. V.; Petrelli, R.; Piergentili, A.; Fontana, S.; Mammoli, V.; Yano, H. 1-[3-(4-Butylpiperidin-1-yl) propyl]-1, 2, 3, 4-tetrahydroquinolin-2-one (77-LH-28-1) as a Model for the Rational Design of a Novel Class of Brain Penetrant Ligands with High Affinity and Selectivity for Dopamine D4 Receptor. *Journal of medicinal chemistry* 2018, 61, 3712-3725.

[5]. Note. The results presented here are obtained from what is now a routinary procedure. For this reason, we built a general model for the paper's structure. This model contains *standard* phrases for the presentation of the methods, calculations and results because they do not need to be rewritten repeatedly and the number of possible variations to use is finite. In 2019.

[6]. Gómez-Jeria, J. S. 45 Years of the KPG Method: A Tribute to Federico Peradejordi. *Journal of Computational Methods in Molecular Design* 2017, 7, 17-37.

[7]. Gómez-Jeria, J. S.; Kpotin, G. Some Remarks on The Interpretation of The Local Atomic Reactivity Indices Within the Klopman-Peradejordi-Gómez (KPG) Method. I. Theoretical Analysis. *Research Journal of Pharmaceutical, Biological and Chemical Sciences* 2018, 9, 550-561.

[8]. Gómez-Jeria, J. S. A New Set of Local Reactivity Indices within the Hartree-Fock-Roothaan and Density Functional Theory Frameworks. *Canadian Chemical Transactions* 2013, 1, 25-55.

[9]. Gómez-Jeria, J. S. *Elements of Molecular Electronic Pharmacology (in Spanish)*. 1st ed.; Ediciones Sokar: Santiago de Chile, 2013; p 104.

[10]. Alarcón, D. A.; Gatica-Díaz, F.; Gómez-Jeria, J. S. Modeling the relationships between molecular structure and inhibition of virus-induced cytopathic efects. Anti-HIV and anti-H1N1 (Influenza) activities as examples. *Journal of the Chilean Chemical Society* 2013, 58, 1651-1659.

[11]. Bruna-Larenas, T.; Gómez-Jeria, J. S. A DFT and Semiempirical Model-Based Study of Opioid Receptor Affinity and Selectivity in a Group of Molecules with a Morphine Structural Core. *International Journal of Medicinal Chemistry* 2012, 2012 Article ID 682495, 1-16.

[12]. Gómez-Jeria, J. S. Modeling the Drug-Receptor Interaction in Quantum Pharmacology. In *Molecules in Physics, Chemistry, and Biology*, Maruani, J., Ed. Springer Netherlands: 1989; Vol. 4, pp 215-231.

[13]. Gómez-Jeria, J. S. On some problems in quantum pharmacology I. The partition functions. *International Journal of Quantum Chemistry* 1983, 23, 1969-1972.

[14]. Statsoft. *Statistica v. 8.0*, 2300 East 14 th St. Tulsa, OK 74104, USA, 1984-2007.

[15]. Gómez-Jeria, J. S. Tables of proposed values for the Orientational Parameter of the Substituent. II. *Research Journal of Pharmaceutical, Biological and Chemical Sciences* 2016, 7, 2258-2260.

[16]. Gómez-Jeria, J. S. Tables of proposed values for the Orientational Parameter of the Substituent. I. Monoatomic, Diatomic, Triatomic, n-CnH2n+1, O-n-CnH2n+1, NRR', and Cycloalkanes (with a single ring) substituents. *Research Journal of Pharmaceutical, Biological and Chemical Sciences* 2016, 7, 288-294.

[17]. Gómez-Jeria, J. S.; Ojeda-Vergara, M. Parametrization of the orientational effects in the drug-receptor interaction. *Journal of the Chilean Chemical Society* 2003, 48, 119-124.

[18]. Kpotin, G. A.; Bédé, A. L.; Houngue-Kpota, A.; Anatovi, W.; Kuevi, U. A.; Atohoun, G. S.; Mensah, J.-B.; Gómez-Jeria, J. S.; Badawi, M. Relationship between electronic structures and antiplasmidial activities of xanthone derivatives: A 2D-QSAR approach. *Structural Chemistry* 2019, In press.

[19]. Gómez-Jeria, J. S.; Sánchez-Jara, B. An introductory theoretical investigation of the relationships between electronic structure and A1, A2A and A3 adenosine receptor affinities of a series of N6-8,9-trisubstituted purine derivatives. *Chemistry Research Journal* 2019, 4, 46-59.

[20]. Gómez-Jeria, J. S.; Gatica-Díaz, N. A preliminary quantum chemical analysis of the relationships between electronic structure and 5-HT_{1A} and 5-HT_{2A} receptor affinity in a series of 8-acetyl-7-hydroxy-4-methylcoumarin derivatives. *Chemistry Research Journal* 2019, 4, 85-100.

[21]. Abdussalam, A.; Gómez-Jeria, J. S. Quantum Chemical Study of the Relationships between Electronic Structure and Corticotropin-Releasing Factor 1 Receptor Binding Inhibition by a Group of Benzazole Derivatives. *Journal of Pharmaceutical and Applied Chemistry* 2019, 5, 1-9.

[22]. Kpotin, G.; Gómez-Jeria, J. S. Quantum-Chemical Study of the Relationships between Electronic Structure and Anti-Proliferative Activities of Quinoxaline Derivatives on the K562 and MCF-7 Cell Lines. *Chemistry Research Journal* 2018, 3, 20-33.

[23]. Frisch, M. J.; Trucks, G. W.; Schlegel, H. B.; Scuseria, G. E.; Robb, M. A.; Cheeseman, J. R.; Montgomery, J., J.A.; Vreven, T.; Kudin, K. N.; Burant, J. C.; Millam, J. M.; Iyengar, S. S.; Tomasi, J.; Barone, V.; Mennucci, B.; Cossi, M.; Scalmani, G.; Rega, N. *G03 Rev. E.01*, Gaussian: Pittsburgh, PA, USA, 2007.

[24]. Gómez-Jeria, J. S. *D-Cent-QSAR: A program to generate Local Atomic Reactivity Indices from Gaussian 03 log files. v. 1.0*, v. 1.0; Santiago, Chile, 2014.

[25]. Gómez-Jeria, J. S. An empirical way to correct some drawbacks of Mulliken Population Analysis (Erratum in: J. Chil. Chem. Soc., 55, 4, IX, 2010). *Journal of the Chilean Chemical Society* 2009, 54, 482-485.